# Modifier clustering and avoidance principle in borosilicate glasses: A molecular dynamics study

Cite as: J. Chem. Phys. **150**, 044502 (2019); https://doi.org/10.1063/1.5051746 Submitted: 12 August 2018 . Accepted: 02 January 2019 . Published Online: 23 January 2019

Mengyi Wang 🗓, Morten M. Smedskjaer, John C. Mauro 🗓, and Mathieu Bauchy 🗓







# ARTICLES YOU MAY BE INTERESTED IN

Cooling rate effects in sodium silicate glasses: Bridging the gap between molecular dynamics simulations and experiments

The Journal of Chemical Physics 147, 074501 (2017); https://doi.org/10.1063/1.4998611

Generalized single-parameter aging tests and their application to glycerol The Journal of Chemical Physics 150, 044501 (2019); https://doi.org/10.1063/1.5066387

Structural, vibrational, and elastic properties of a calcium aluminosilicate glass from molecular dynamics simulations: The role of the potential

The Journal of Chemical Physics 141, 024507 (2014); https://doi.org/10.1063/1.4886421





# Modifier clustering and avoidance principle in borosilicate glasses: A molecular dynamics study

Cite as: J. Chem. Phys. 150, 044502 (2019); doi: 10.1063/1.5051746 Submitted: 12 August 2018 · Accepted: 2 January 2019 · Published Online: 23 January 2019







Mengyi Wang, 12 D Morten M. Smedskjaer, 3 John C. Mauro, 4 D and Mathieu Bauchy 1 D



# **AFFILIATIONS**

- Physics of AmoRphous and Inorganic Solids Laboratory (PARISIab), Department of Civil and Environmental Engineering, University of California, Los Angeles, California 90095, USA
- <sup>2</sup>Department of Materials Science and Engineering, Massachusetts Institute of Technology, Cambridge, Massachusetts 02139, USA
- Department of Chemistry and Bioscience, Aalborg University, 9220 Aalborg, Denmark
- Department of Materials Science and Engineering, The Pennsylvania State University, University Park, Pennsylvania 16802, USA

#### **ABSTRACT**

Oxide glasses are typically described as having a random, disordered skeleton of network-forming polyhedra that are depolymerized by network-modifying cations. However, the existence of local heterogeneity or clustering within the network-forming and network-modifying species remains unclear. Here, based on molecular dynamics simulations, we investigate the atomic structure of a series of borosilicate glasses. We show that the network-modifying cations exhibit some level of clustering that depends on composition-in agreement with Greaves' modified random network model. In addition, we demonstrate the existence of some mutual avoidance among network-forming atoms, which echoes the Loewenstein avoidance principle typically observed in aluminosilicate phases. Importantly, we demonstrate that the degree of heterogeneity in the spatial distribution of the network modifiers is controlled by the level of ordering in the interconnectivity of the network formers. Specifically, the mutual avoidance of network formers is found to decrease the propensity for modifier clustering.

Published under license by AIP Publishing. https://doi.org/10.1063/1.5051746

#### I. INTRODUCTION

Borosilicate glasses have various applications, including kitchen and laboratory glassware, 1,2 glass fibers,3 chemically strengthened protective cover glasses,4-6 glass substrates for high-performance displays,7 and nuclear waste immobilization.8-10 However, our ability to develop new borosilicate glass formulations featuring improved properties is largely hindered by the lack of knowledge of their atomic structure.1

Since the pioneering studies of Zachariasen and Sun, the atomic network of oxide glasses is traditionally described as a rigid skeleton of network-forming atoms (e.g., Si or B), which is partially depolymerized and/or charge-compensated by network-modifying species (e.g., Na or Ca). 12-14 The networkforming skeleton of borosilicate glasses is partially derived from those of pure glassy SiO<sub>2</sub> and B<sub>2</sub>O<sub>3</sub>.<sup>14</sup> The atomic network of SiO2 consists of SiO4 tetrahedra that are interconnected through their corners by bridging oxygen (BO) atoms. The structure of pure B<sub>2</sub>O<sub>3</sub> glass is, at the short-range order scale, composed of triangular BO3 structural units connected by BOs at their corners. Starting from these basic topologies, the introduction of network modifiers can have different effects. Specifically, each alkali cation M may associate with either (i) Si or B to create a non-bridging oxygen (NBO) atom or (ii) with B to convert boron from a trigonal BO3 unit to a BO<sub>4</sub> tetrahedral unit by acting as a charge compensator. While the latter mechanism is typically predominant at M/B < 0.5, both mechanisms can coexist. 15 The effect of alkalineearth cations R is typically equivalent to that of two alkali cations, i.e., they can form two NBOs and stabilize two BO4 units.16

Building largely on nuclear magnetic resonance spectroscopy studies,<sup>17</sup> much is known about the short-range topology of oxide glasses. However, the extent of order and disorder in the distribution of the network-forming and network-modifying species remains poorly known.<sup>18</sup> First, there remains some debate whether the network-modifying species are homogeneously distributed throughout the glass or if they exhibit some microsegregation-as predicted by Greaves' modified random network model. 19,20 The existence of modifier clustering is an important question as it would affect the mobility of the modifiers and could act as a precursor for phase separation. 18,21,22 Second, the degree of randomness in the mutual connectivity among network-forming species is also unclear. For instance, aluminosilicate glasses have been suggested to partially satisfy Loewenstein's rule (or Al exclusion principle), which states that AlO<sub>4</sub>-SiO<sub>4</sub> interpolytope linkages preferentially form, at the expense of AlO<sub>4</sub>-AlO<sub>4</sub> connections.<sup>23</sup> The degree of mixing among Si and B atoms in borosilicate glasses has also been linked to their propensity for phase separation.<sup>24,25</sup> All these questions interrogate the random or partially ordered nature of the atomic network of oxide glasses.

Here, based on molecular dynamics (MD) simulations of a series of sodium–calcium borosilicate glasses with varying compositions, we investigate the distribution and interconnectivity of the network-forming and network-modifying species. We show that the level of order and disorder in modifier clustering depends on the composition of the glass. In addition, some degree of mutual avoidance among boron atoms is also observed. We demonstrate that, in borosilicate glasses, these two behaviors are closely related to each other as the mutual avoidance among network formers decreases the propensity for modifier clustering.

# **II. SIMULATION METHODOLOGY**

# A. Glass compositions

To establish our conclusions, we conduct some classical MD simulations of a series of borosilicate glasses, whose compositions and naming are presented in Table I. This list comprises a series of borosilicate glasses with varying Si/B molar ratios at fixed network modifier content (namely, 15 mol. % Na<sub>2</sub>O and 10 mol. % CaO). The glasses are named

TABLE I. Compositions of the glasses simulated herein.<sup>27</sup>

	Chemical composition (mol. %)				
Glass ID	SiO <sub>2</sub>	B <sub>2</sub> O <sub>3</sub>	Na <sub>2</sub> O	CaO	
75B	0	75	15	10	
62B	13	62	15	10	
50B	25	50	15	10	
37B	38	37	15	10	
24B	51	24	15	10	
12B	63	12	15	10	
6B	69	6	15	10	
0B	75	0	15	10	

75B-0B, ranging from modified borates to modified silicates. These glasses are selected as they have been extensively characterized experimentally by Smedskjaer, Mauro, and Yue.11.26

#### B. Empirical potential

Simulations of borosilicate glasses are traditionally challenging due to the variable nature of the coordination number of B atoms (i.e., 3- or 4-fold coordinated). To investigate the structure of the glasses considered herein, we rely on a new interatomic force field that we recently developed for borosilicate systems.<sup>27</sup> The potential is an extension of the force field initially developed by Guillot and Sator, which has been proven to show an excellent transferability over a wide range of modified silicate minerals and glasses while retaining constant parameters.<sup>28-30</sup> The potential only comprises two-body Buckingham potential energy terms

$$U_{ij}(r_{ij}) = \frac{z_i z_j}{r_{ij}} + A_{ij} \exp\left(\frac{-r_{ij}}{\rho_{ij}}\right) - \frac{C_{ij}}{r_{ij}^6}, \tag{1}$$

where  $r_{ij}$  is the distance between the atoms i and j,  $z_i$  is the effective partial charge of atom i, and  $A_{ij}$ ,  $\rho_{ij}$ , and  $C_{ij}$  are the energy parameters for the pair of atoms (i, j). The energy terms correspond to the Coulombic interactions, short-range electronic repulsion, and van der Waals interactions, respectively. Note that, unlike previous potentials developed for borosilicate systems,<sup>31</sup> all the parameters are fixed and independent of composition. The effective partial charges and potential parameters are given in Tables II and III, respectively-note that only electrostatic interactions are considered for all the pairs that are not listed (e.g., B-Na). In general, an additional short-range repulsive term of the form  $U(r) = B/r^n$ might be needed to avoid the "Buckingham catastrophe" at high temperature. 32,33 However, such a term is not needed here as the simulated systems exhibit a low glass transition temperature—so that an initial temperature as low as 3000 K is high enough to fully randomize the initial configuration within a few picoseconds.

TABLE II. Fixed partial charge attributed to each element.<sup>27</sup>

Element	Partial charge (e)	
0	-0.945	
Si	1.89	
В	1.4175	
Ca	0.945	
Na	0.4725	
Ti <sup>a</sup>	1.89	
Ala	1.4175	
Fe <sup>3+a</sup>	1.4175	
Fe <sup>2+a</sup>	0.945	
${f Fe^{3+a}} \ {f Fe^{2+a}} \ {f Mg^a} \ {f K}^a$	0.945	
Ka	0.4725	

<sup>&</sup>lt;sup>a</sup>These parameters are sourced from the original Guillot–Sator interatomic potential. <sup>28</sup> They are indicated herein for reference, although these elements are not considered in the present study.

**TABLE III.** Parameters of the interatomic potential.<sup>27</sup>

Bond	A <sub>ij</sub> (eV)	$ ho_{ij}$ (Å)	C <sub>ij</sub> (eV Å <sup>6</sup> )
0-0	9 022.79	0.265	85.0921
Si-O	50 306.10	0.161	46.2978
В-О	206 941.81	0.124	35.0018
B-B	484.40	0.35	0.0
Si-B	337.70	0.29	0.0
Na-O	120 303.80	0.17	0.0
Ca-O	155 667.70	0.178	42.2597
Ti-O <sup>a</sup>	50126.64	0.178	46.2978
Al-O <sup>a</sup>	28 538.42	0.172	34.5778
Fe <sup>3+</sup> -O <sup>a</sup>	8 020.27	0.19	0.0
Fe <sup>2+</sup> -O <sup>a</sup>	13 032.93	0.19	0.0
Mg-O <sup>a</sup>	32 652.64	0.178	27.2810
K-O <sup>a</sup>	2 284.77	0.29	0.0

<sup>&</sup>lt;sup>a</sup>These parameters are sourced from the original Guillot–Sator interatomic potential. <sup>28</sup> They are indicated herein for reference, although these elements are not considered in the present study.

#### C. Simulation details

All simulations are conducted using the LAMMPS package.34 We use a cutoff of 11 Å both for the short-range and Coulombic interactions. The long-range Coulombic interactions are calculated with the particle-particle particlemesh (PPPM) algorithm with an accuracy of  $10^{-5}$ . The time step is fixed at 1.0 fs. The glasses are simulated using the traditional melt-quench procedure, as described in the following. 32,35,36 First, around 3000 atoms are randomly placed within a cubic box while ensuring the absence of any unrealistic overlap. The system is then melted at 3000 K in the canonical (NVT) ensemble for 10 ps and at zero pressure (NPT ensemble) for 100 ps, which ensures a complete loss of the memory of the initial configuration. The system is subsequently cooled linearly to 300 K at zero pressure (NPT ensemble) with a cooling rate of 1 K/ps. All of the resulting glasses are further relaxed at 300 K and zero pressure for 100 ps before a final NVT run of 100 ps for statistical averaging. In the following, all properties referring to the "glassy state" are averaged over 100 configurations extracted with an interval of 1 ps from this run.

In specific cases, we observe that initial configurations with unrealistic structure tend to "explode" (i.e., their volume indefinitely increases over time) at high temperature in the NPT ensemble. In such cases, we first create a more realistic structure by melting the initial configuration at 3000 K in the NVT ensemble for 100 ps and then cooling the system linearly to 300 K at fixed volume (NVT ensemble). The obtained glassy structure is then used as the starting configuration for the melt-quench procedure previously described.

# D. Validation of the potential

Figure 1(a) shows the computed density values for the series of borosilicate glasses considered herein (see Table I). We observe that the glass density gradually increases with increasing SiO<sub>2</sub> concentration, reaches a maximum at around  $[B_2O_3]/([SiO_2]+[B_2O_3]) = 0.3$ , and eventually decreases at high amount of SiO<sub>2</sub>. The maximum of density was found to arise from a minimum in the average borosilicate ring size.<sup>27</sup> Figure 1(b) shows the fraction of 4-fold coordinated B atoms, which is found to decrease monotonically with increasing B<sub>2</sub>O<sub>3</sub> concentration. This can be understood from the fact that, at high amount of B<sub>2</sub>O<sub>3</sub> (i.e., low amount of SiO<sub>2</sub>), there is a deficit of Na and Ca cations as compared to the large number of B atoms so that only a small fraction of the B atoms can be charge-compensated and form BO<sub>4</sub> units. On the other hand, at a low amount of B<sub>2</sub>O<sub>3</sub> (i.e., high amount of SiO<sub>2</sub>), there is a large excess of Na and Ca atoms so that the majority of the B atoms tend to form charge-compensated BO<sub>4</sub> units. It is worth noting that, however realistic the force field may be, MD simulations come with some intrinsic limitations. For instance, the high cooling rate typically results in a glass structure that is more disordered than in experiments. As such, select structural features (e.g., B-NBO bonds) may be an artifact of MD simulations. Nevertheless, all the data presented in Fig. 1 are in excellent agreement with experimental data-both in terms of trend and absolute value 11-which demonstrates the ability of the present potential to offer a realistic description of the structure of modified borosilicate glasses. An extensive validation of the structure and

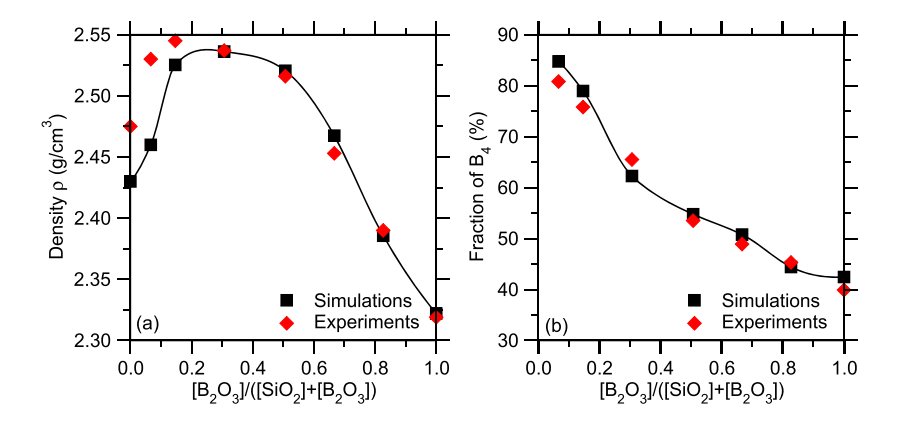


FIG. 1. Computed (a) density and (b) fraction of 4-fold coordinated B cations, compared with experimental data. 11.27 Error bars are smaller than the size of the symbols. The line is a guide to the eye.

properties of the simulated borosilicate glasses can be found in Ref. 27.

## III. RESULTS

#### A. Local environment of the modifiers

We first assess the local atomic environment of the network-modifying species (namely, Ca and Na). Figure 2 shows the computed partial Ca–O and Na–O pair distribution functions (PDFs). Overall, we observe that the local environment of the network modifiers significantly depends on the glass composition. In both cases, we observe that the interatomic bond distance increases upon the addition of B<sub>2</sub>O<sub>3</sub>. This suggests that the Ca–O and Na–O bond distances are larger when Ca and Na act as charge-compensators (i.e., to compensate the charge of negatively charged BO<sub>4</sub> tetrahedral units) than when they act as network-modifiers (i.e., to create NBOs). This can be understood from the fact that Ca and Na cations are more strongly bonded to the created NBO(s) than to the surrounding BOs when they act as charge-compensators [see Fig. 2(c)].<sup>38</sup>

We now further describe the mechanism of charge compensation that enables the formation of 4-fold B atoms. Figure 3 shows the computed fractions of 4-fold B atoms that are charge-compensated by Ca and Na cations, respectively, wherein, for each 4-fold B atom, the charge-compensating cation is determined as being the network modifier that is the closest from the central B atom. Note that the existence of a small fraction of B<sup>4</sup>-NBO bonds (which may be an artifact from the high cooling rate used in MD simulations) may partially affect these results. Overall, we observe that a majority of 4-fold coordinated B units are charge-compensated by Na cations. This is not surprising as all the simulated glasses comprise more Na than Ca cations (see Table I).

To better characterize the type of charge-compensation scheme that is favored within the glass, the computed data presented in Fig. 3 are compared to the predictions of a random model, that is, where each BO<sub>4</sub> can randomly pick a

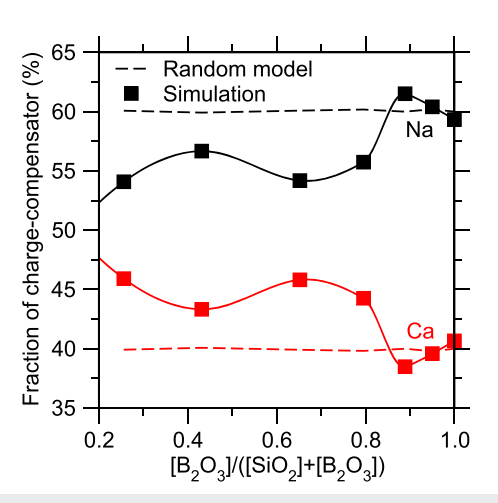


**FIG. 3**. Computed fractions of the 4-fold coordinated B atoms that are charge-compensated by Ca and Na cations. The solid line is a guide to the eye. The dashed lines indicate the results calculated by assuming a random model [see Eq. (2)].

 ${
m Ca^{2+}}$  or  ${
m Na^{+}}$  cation to compensate their local charge. Note that each  ${
m Ca^{2+}}$  and  ${
m Na^{+}}$  cations can compensate 2 and 1 BO<sub>4</sub> units, respectively. The fractions of 4-fold B units charge-compensated by Ca and Na cations (denoted  $f_{
m Ca}$  and  $f_{
m Na}$ , respectively) that are predicted by this random model are given by

$$f_{\text{Ca}} = \frac{2N_{\text{Ca}}}{2N_{\text{Ca}} + N_{\text{Na}}}, \quad f_{\text{Na}} = \frac{N_{\text{Na}}}{2N_{\text{Ca}} + N_{\text{Na}}},$$
 (2)

where  $N_{Ca}$  and  $N_{Na}$  are the number of Ca and Na atoms in the system, respectively. Note that, here, no attempt is made to discriminate the cations that compensate  $BO_4$  units from those that create NBOs—as we find in our simulations that some Ca and Na cations are simultaneously close to  $BO_4$  units and NBOs, which renders challenging a meaningful distinction between network–modifying and charge-compensating

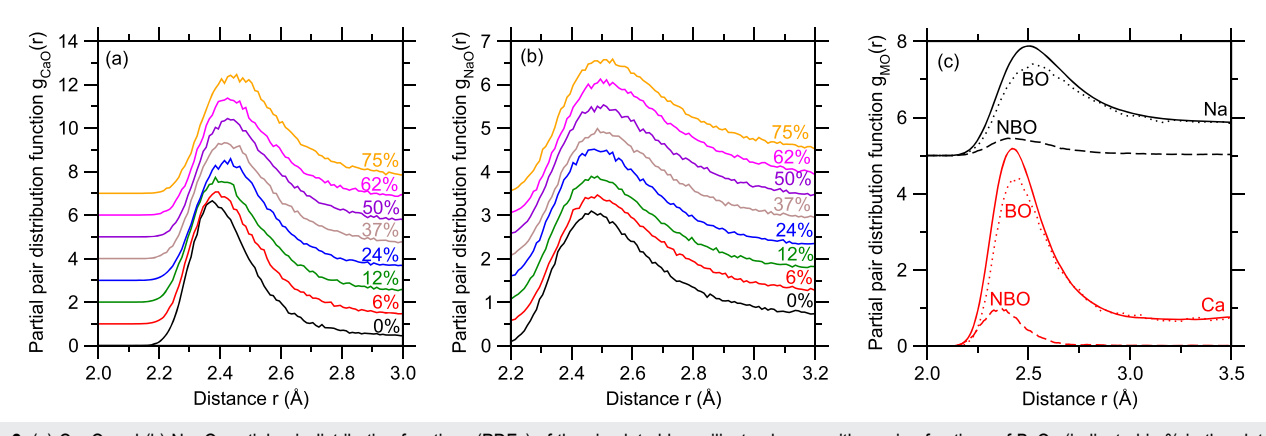


FIG. 2. (a) Ca–O and (b) Na–O partial pair distribution functions (PDFs) of the simulated borosilicate glasses with varying fractions of B<sub>2</sub>O<sub>3</sub> (indicated in % in the plot, see Table I). (c) Contributions of BO and NBO atoms to the Ca–O and Na–O partials PDFs for [B<sub>2</sub>O<sub>3</sub>] = 37%.

cations at the atomic level. As shown in Fig. 3, we observe that most glasses exhibit an excess of Ca and a deficit of Na charge-compensators with respect to the predictions of the random models. This suggests that, for the glasses considered herein, BO<sub>4</sub> units are preferentially charge-compensated by Ca rather than by Na cations. This result contrasts with findings obtained in aluminosilicate and borosilicate glasses.<sup>39,40</sup> By contrast, at high amount of B<sub>2</sub>O<sub>3</sub>, we observe that the distributions that are computed and predicted by the random model become comparable. This can be understood from the fact that, in B-rich glasses, there are not enough Ca and Na cations to compensate the charge of all the BO<sub>4</sub> units. As such, all cations are used as charge compensators—so that the distributions are fully determined by the number of Ca and Na cations available in the glass.

## B. Clustering of the modifiers

We now investigate the spatial organization of the network-modifying species. Figure 4 shows the computed partial Ca–Ca, Na–Na, and Ca–Na PDFs. In all the pair distribution functions, we observe the existence of a well-defined correlation peak around 3.5, 3.1, and 3.4 Å for Ca–Ca, Na–Na, and Ca–Na cations pairs, respectively. This peak suggests the existence of some spatial correlations among Ca and Na cations and suggests that Ca and Na cations tend to cluster within pockets or channels. However, we note that the propensity for cation agglomeration decreases upon the addition of  $B_2O_3$ , as the intensity of the correlation peak tends to decrease.

We further analyze the spatial distribution of the modifiers by computing the average distance between nearest pairs of Ca and Na modifiers (see Fig. 5). We observe that, on average, the average distance between Na–Na clusters is shorter than that observed for Ca–Ca clusters which is in agreement with the fact that first peak of the Ca–Ca PDF is located at higher distance than that of the Na–Na PDF. We note that, for both types of cations, the average distance between

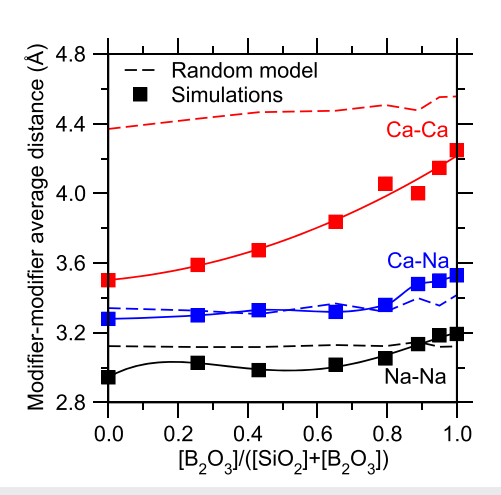


**FIG. 5.** Computed average M–M distance (when M = Ca and Na) in borosilicate glasses with varying B/Si molar ratios (see Table I). The solid lines are a guide to the eye. The dashed lines indicate the average M–M distance calculated by assuming a random distribution of the modifiers.

nearest pairs of modifiers is increasing upon the addition of  $B_2O_3$ .

To better quantify the degree of clustering among the network modifiers, the data presented in Fig. 5 are compared with the predictions of a random model, wherein the modifiers are randomly distributed throughout the simulation box while ensuring the absence of any unrealistic overlap. Overall, we observe that the average distance between nearest pairs of modifiers is systematically lower than that predicted by the random model, which demonstrates the existence of some clustering within the network-modifying species. We note that the degree of clustering (i.e., the departure from the random model) is more pronounced for Ca than for Na cations. However, in both cases, the degree of clustering is found to decrease upon the addition of  $B_2O_3$  as both Ca-Ca and Na-Na distances become closer to that

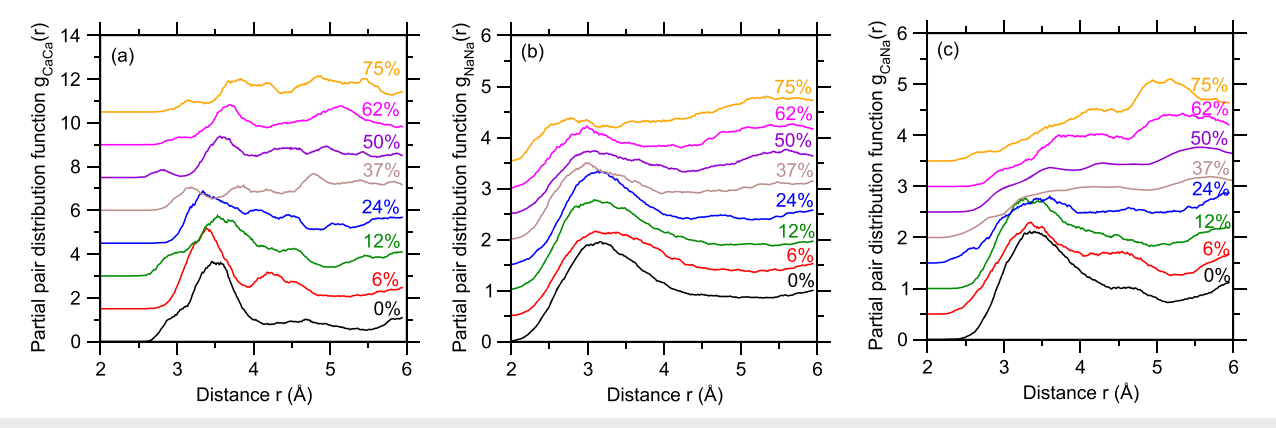


FIG. 4. (a) Ca–Ca, (b) Na–Na, and (c) Ca–Na partial pair distribution functions of the simulated borosilicate glasses with varying fractions of  $B_2O_3$  (indicated in % in the plot, see Table I).

predicted by the random model. This suggests that the addition of  $B_2O_3$  effectively induces the homogenization of the network modifiers. By contrast, we observe that the average distance between nearest Ca–Na pairs is fairly close to the predictions of the random model. This suggests that Ca and Na cations form distinct clusters and do not show any notable propensity to mix with each other (or avoid each other).

#### C. Mutual avoidance of the network-forming species

We now place our attention on the interpolytope connectivity among the network-forming species. Figure 6 shows the fractions of Si–O–Si, Si–O–B, and B–O–B linkages as a function of composition. As expected, we observe that the fractions of Si–O–Si and B–O–B connections increase with the SiO $_2$  and B $_2$ O $_3$  concentrations, respectively. In between, the fraction of Si–O–B exhibits a maximum when the numbers of B and Si atoms are equal to each other.

To quantify the level of order and disorder in the interpolytope connectivity, the computed data presented in Fig. 6 are compared to the predictions of a random model, wherein each network former can randomly pick its Si or B neighbors. This model accounts for the composition-dependent coordination number of B atoms. According to this model, the fractions of Si-O-Si, Si-O-B, and B-O-B bonds are given by

$$f_{\text{Si-O-Si}} = \frac{4N_{\text{Si}} \times 4N_{\text{Si}}}{(4N_{\text{Si}} + 3N_{\text{BIII}} + 4N_{\text{BIV}})^{2}},$$

$$f_{\text{Si-O-B}} = \frac{2 \times 4N_{\text{Si}} \times (3N_{\text{BIII}} + 4N_{\text{BIV}})}{(4N_{\text{Si}} + 3N_{\text{BIII}} + 4N_{\text{BIV}})^{2}},$$

$$f_{\text{B-O-B}} = \frac{3N_{\text{BIII}} \times 3N_{\text{BIII}} + 2N_{\text{BIV}}}{(4N_{\text{Si}} + 3N_{\text{BIII}} + 4N_{\text{BIV}})^{2}},$$

$$(3)$$

where  $N_{Si}$ ,  $N_{BIII}$ , and  $N_{BIV}$  are the numbers of Si, 3-fold, and 4-fold B atoms, respectively. As shown in Fig. 6, we observe a

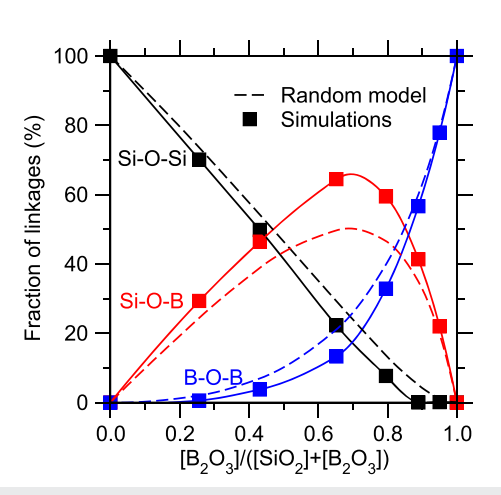


**FIG. 6.** Computed distribution of the Si–O–Si, Si–O–B, and B–O–B interpolytope linkages. The solid lines are a guide to the eye. The dashed lines indicate the fractions of each type of inter-polytope linkage calculated by assuming a random model [see Eq. (3)].

significant excess of asymmetric Si-O-B linkages at the expense of symmetric Si-O-Si and B-O-B bonds with respect to the predictions of the random model, which closely echoes previous experimental results.<sup>24,41</sup> These results show that there is a propensity for B atoms to avoid each other when combined with Si atoms. This suggests the existence of a "boron avoidance principle" in borosilicate glasses that is similar to the Loewenstein aluminum avoidance principle observed in aluminosilicate glasses.<sup>23,35</sup>

To further investigate the origin of the mutual avoidance among B atoms, we now assess the influence of the coordination number of B on its polytope neighbors. Figure 7 shows the fractions of B<sup>III</sup>–O–B<sup>III</sup>, B<sup>III</sup>–O–B<sup>IV</sup>, and B<sup>IV</sup>–O–B<sup>IV</sup> linkages. We first observe that Gupta's random pair model (wherein BO<sub>4</sub> units are assumed to form some dimers that are isolated from

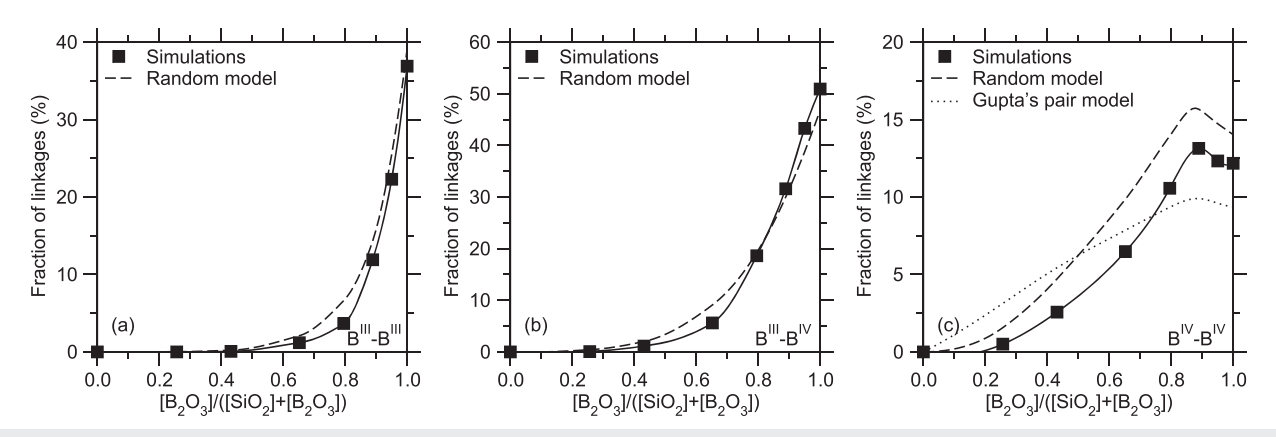


FIG. 7. Computed fractions of (a) B<sup>III</sup>–B<sup>III</sup>, (b) B<sup>III</sup>–B<sup>IV</sup>, and (c) B<sup>IV</sup>–B<sup>IV</sup> inter-polytope linkages, where B<sup>III</sup> and B<sup>IV</sup> denote the 3- and 4-fold coordinated B atoms, respectively. The solid lines are a guide to the eye. The dashed lines indicate the fraction of each type of inter-polytope linkage calculated by assuming a random model [see Eq. (3)]. The dotted line is the prediction from Gupta's random pair model. 42.43

each other 42,43) offers a reasonable prediction of the fraction of B<sup>IV</sup>-O-B<sup>IV</sup> linkages [see Fig. 7(c)], although this model tends to overestimate and underestimate the fraction of such bonds for low and high amounts of B2O3, respectively. Furthermore, by comparing the fractions of each type of bonds to the predictions of the random model [see Eq. (3)], we observe that the mutual avoidance among B atoms mostly arises from a deficiency of B<sup>IV</sup>-O-B<sup>IV</sup> bonds. The mutual avoidance between BO<sub>4</sub> tetrahedral units that is evidenced herein has been suggested in previous experimental studies.<sup>24,44,45</sup> This mutual avoidance can be explained from the fact that BO<sub>4</sub> units exhibit a local charge of -1 (i.e., they need a cation acting as charge compensator in their vicinity) and, hence, their mutual connection should indeed be energetically unfavorable due to mutual Columbic repulsion. Altogether, these results echo the Loewenstein Al-avoidance principle observed in aluminosilicate glasses comprising 4-fold coordinated Al atoms. 23,35

#### IV. DISCUSSION

Altogether, these results suggest that the clustering of network modifiers and the avoidance among network formers are closely related to each other. First, we note that when only one type of network-forming species is present in the network (i.e., for pure silicate glasses here), a significant propensity for modifier clustering is observed. This suggests that such clustering is intrinsic to silicate glasses. Second, we observe that the propensity for clustering decreases when different types of network-forming species coexist (i.e., in mixed Si-B glasses or in borate glasses, wherein 3- and 4-fold B units coexist). The degree of mutual avoidance among BO4 tetrahedral units has been noted to depend on the type of network modifier present in the glass structure, which suggests a close correlation between the distributions of the network-forming and network-modifying species. 46 Namely, the loss of clustering is likely to arise from the mutual avoidance among network formers, which favors homogeneity. Indeed, at high B<sub>2</sub>O<sub>3</sub> concentration, the modifiers act as charge-compensators and, therefore, stay in the vicinity of BO<sub>4</sub> units. Hence, an increase in the homogeneity of BO<sub>4</sub> units (i.e., due to their mutual avoidance) should effectively prevent the clustering of their charge-compensating cations. In addition, at lower B<sub>2</sub>O<sub>3</sub> concentration, it has been suggested that NBOs are preferentially connected to Si than B units. 11 Hence, the fact that asymmetric Si-O-B bonds are favored tends to increase the average distance among Si atoms and, thereby, should prevent the formation of clusters of network-modifying species.

It is worth noting that the propensity for network modifier clustering and avoidance among network former is likely to strongly depend on the thermal history (e.g., the cooling rate) of the glass, although this effect has not been investigated herein. Since glasses simulated by MD are typically more random than real glasses due to the high cooling rate used in simulations, <sup>32,47</sup> one can expect that the extent of atomic-scale heterogeneity in oxide glasses might be even more pronounced than what the present simulation results suggest. Such heterogeneity might eventually result in extended phase

separation—the slow kinetics of which being inaccessible to traditional MD simulations. Note that all the glasses simulated herein have been found to be optically transparent and inspection under cross-polarized light showed no evidence of phase separation. However, it is worth noting that one may not exclude the existence of some nanoscale phase separation—which often remains undetected as it does not impact glass transparency. 48,49

#### V. CONCLUSIONS

Based on MD simulations of a series of borosilicate glasses, we have shown that modifier clustering is an intrinsic feature of silicate glasses. Nevertheless, the propensity for such clustering decreases when distinct types of networkforming species are present in the network. As such, the presence of mixed network formers effectively favors the homogeneity of the atomic network. Our simulations also reveal the existence of a boron avoidance principle, wherein mutual connections among 4-fold coordinated B units are avoided-which is analogous to the aluminum avoidance principle observed in aluminosilicate glasses. Overall, these results suggest that the degree of local heterogeneity in the distributions of the network formers and modifiers are closely correlated. More generally, this study also highlights the fact that, even in the absence of any microstructural phase separation, oxide glasses are not fully random at the atomic scale-a consequence of the competition between energetic and entropic effects upon cooling.

# SUPPLEMENTARY MATERIAL

See supplementary material for some tabulated data regarding the structure of the borosilicate glasses simulated herein.

#### **ACKNOWLEDGMENTS**

This work was partially funded by Corning Incorporated and the National Science Foundation under Grant Nos. 1762292 and 1826420. M.M.S. acknowledges support from the Independent Research Fund Denmark (Grant No. 7017-00019).

# **REFERENCES**

- <sup>1</sup>J. C. Phillips and R. Kerner, J. Chem. Phys. **128**, 174506 (2008).
- <sup>2</sup>M. M. Smedskjaer, R. E. Youngman, and J. C. Mauro, Appl. Phys. A 116, 491 (2014).
- <sup>3</sup> Borate Glasses, edited by L. D. Pye, V. D. Fréchette, and N. J. Kreidl (Springer US, Boston, MA, 1978).
- <sup>4</sup>P. Ball, Nat. Mater. **14**, 472 (2015).
- <sup>5</sup>J. C. Mauro, A. J. Ellison, and L. D. Pye, Int. J. Appl. Glass Sci. **4**, 64 (2013).
- <sup>6</sup>J. C. Mauro and M. M. Smedskjaer, Phys. A **391**, 6121 (2012).
- <sup>7</sup>A. Ellison and I. A. Cornejo, Int. J. Appl. Glass Sci. 1, 87 (2010).
- <sup>8</sup>J. D. Vienna, J. V. Ryan, S. Gin, and Y. Inagaki, Int. J. Appl. Glass Sci. 4, 283 (2013)
- <sup>9</sup>M. I. Ojovan and W. E. Lee, An Introduction to Nuclear Waste Immobilisation (Newnes, 2013).

- <sup>10</sup>C. M. Jantzen, K. G. Brown, and J. B. Pickett, Int. J. Appl. Glass Sci. 1, 38 (2010).
- <sup>11</sup> M. M. Smedskjaer, J. C. Mauro, R. E. Youngman, C. L. Hogue, M. Potuzak, and Y. Yue, J. Phys. Chem. B 115, 12930 (2011).
- 12 W. H. Zachariasen, J. Am. Chem. Soc. 54, 3841 (1932).
- <sup>13</sup>K.-H. Sun, J. Am. Ceram. Soc. **30**, 277 (1947).
- <sup>14</sup>A. K. Varshneya, Fundamentals of Inorganic Glasses (Academic Press, Inc., 1993).
- <sup>15</sup>Y. H. Yun and P. J. Bray, J. Non-Cryst. Solids 27, 363 (1978).
- <sup>16</sup>F. Michel, L. Cormier, P. Lombard, B. Beuneu, L. Galoisy, and G. Calas, J. Non-Cryst. Solids 379, 169 (2013).
- <sup>17</sup>M. Edén, Annu. Rep. Prog. Chem., Sect. C: Phys. Chem. **108**, 177 (2012).
- <sup>18</sup>G. N. Greaves and S. Sen, Adv. Phys. **56**, 1 (2007).
- <sup>19</sup>G. N. Greaves, J. Non-Cryst. Solids **71**, 203 (1985).
- <sup>20</sup>B. Vessal, G. N. Greaves, P. T. Marten, A. V. Chadwick, R. Mole, and S. Houde-Walter, Nature 356, 504 (1992).
- <sup>21</sup> M. Bauchy and M. Micoulaut, Phys. Rev. B 83, 184118 (2011).
- <sup>22</sup>G. N. Greaves and K. L. Ngai, Phys. Rev. B 52, 6358 (1995).
- <sup>23</sup>W. Loewenstein, Am. Mineral. **39**, 92 (1954), see https://pubs. geoscienceworld.org/georef/record/6/327529/the-distribution-of-alum inun-in-the-tetrahedra-of.
- <sup>24</sup>L.-S. Du and J. F. Stebbins, J. Phys. Chem. B **107**, 10063 (2003).
- <sup>25</sup>L.-S. Du and J. F. Stebbins, J. Non-Cryst. Solids **315**, 239 (2003).
- <sup>26</sup> M. M. Smedskjaer, J. C. Mauro, and Y. Yue, J. Phys. Chem. B 119, 7106 (2015).
- <sup>27</sup>M. Wang, N. M. Anoop Krishnan, B. Wang, M. M. Smedskjaer, J. C. Mauro, and M. Bauchy, J. Non-Cryst. Solids 498, 294 (2018).
- <sup>28</sup>B. Guillot and N. Sator, Geochim. Cosmochim. Acta 71, 1249 (2007).
- <sup>29</sup> M. Bauchy, B. Guillot, M. Micoulaut, and N. Sator, Chem. Geol. **346**, 47 (2013).
- <sup>30</sup>R. Vuilleumier, N. Sator, and B. Guillot, Geochim. Cosmochim. Acta 73, 6313 (2009).

- <sup>31</sup> L.-H. Kieu, J.-M. Delaye, L. Cormier, and C. Stolz, J. Non-Cryst. Solids 357, 3313 (2011).
- <sup>32</sup>X. Li, W. Song, K. Yang, N. M. A. Krishnan, B. Wang, M. M. Smedskjaer, J. C. Mauro, G. Sant, M. Balonis, and M. Bauchy, J. Chem. Phys. **147**, 074501 (2017).
- 33 J. Du and A. Cormack, J. Non-Cryst. Solids 349, 66 (2004).
- <sup>34</sup>S. Plimpton, J. Comput. Phys. **117**, 1 (1995).
- 35 M. Bauchy, J. Chem. Phys. 141, 024507 (2014).
- <sup>36</sup>M. Bauchy, J. Chem. Phys. **137**, 044510 (2012).
- <sup>37</sup>J. Du, in Molecular Dynamics Simulations of Disordered Materials, edited by C. Massobrio, J. Du, M. Bernasconi, and P. S. Salmon (Springer International Publishing, 2015), pp. 157–180.
- <sup>38</sup>M. Bauchy and M. Micoulaut, J. Non-Cryst. Solids **357**, 2530 (2011).
- <sup>39</sup>S. K. Lee and S. Sung, Chem. Geol. **256**, 326 (2008).
- <sup>40</sup>F. Angeli, T. Charpentier, E. Molières, A. Soleilhavoup, P. Jollivet, and S. Gin, J. Non-Cryst. Solids 376, 189 (2013).
- <sup>41</sup>F. Angeli, T. Charpentier, M. Gaillard, and P. Jollivet, J. Non-Cryst. Solids **354**, 3713 (2008).
- $^{42}\mathrm{P.}$  K. Gupta, in 14th International Congress on Glass, Collected Papers, 1986.
- 43 J. C. Mauro, P. K. Gupta, and R. J. Loucks, J. Chem. Phys. 130, 234503 (2009).
- <sup>44</sup>M. Storek, M. Adjei-Acheamfour, R. Christensen, S. W. Martin, and R. Böhmer, J. Phys. Chem. B **120**, 4482 (2016).
- <sup>45</sup>D. Manara, A. Grandjean, and D. R. Neuville, J. Non-Cryst. Solids **355**, 2528 (2009).
- 46 L.-S. Du and J. F. Stebbins, Chem. Mater. 15, 3913 (2003).
- <sup>47</sup>L. Deng and J. Du, J. Chem. Phys. **148**, 024504 (2018).
- <sup>48</sup>L. Martel, M. Allix, F. Millot, V. Sarou-Kanian, E. Véron, S. Ory, D. Massiot, and M. Deschamps, J. Phys. Chem. C 115, 18935 (2011).
- <sup>49</sup> M. Cavillon, P. Dragic, B. Greenberg, S. H. Garofalini, and J. Ballato, J. Am. Ceram. Soc. 0, 879 (2018).